Questioning the γ-gauche effect: stereoassignment of 1,3-disubstituted-tetrahydro-β-carbolines using [1]H-^{1}H coupling constants
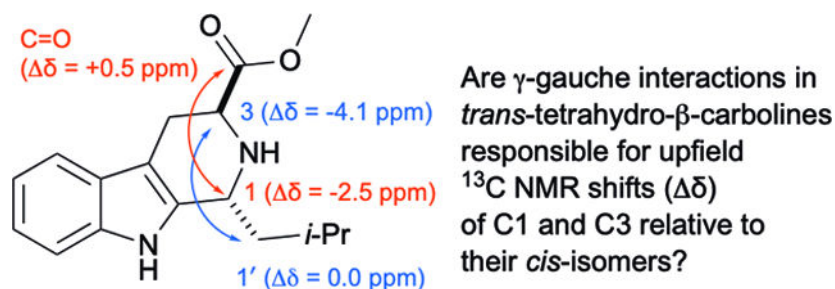
Kristýna Cagašová, **Maryam Ghavami**, **Zhong-Ke Yao**, and **Paul R. Carlier**

Department of Chemistry and Virginia Tech Center for Drug Discovery, Virginia Tech, Hahn Hall South, 800 West Campus Drive, Blacksburg, Virginia 24061, United States.

Abstract

The Pictet-Spengler reaction of tryptophan esters and aldehydes has been widely applied in natural product synthesis and medicinal chemistry. To date, the *trans*- or *cis*-configuration of 1,3-disubstituted tetrahydro-β-carbolines (THβCs) formed in this reaction has most often been assigned based on the relative ^{13}C chemical shifts of C1 and C3 in the diastereomers. Although the upfield shifts of C1 and C3 in *trans*-THβCs relative to *cis*-THβCs has been attributed to steric compression associated with the "γ-gauche" effect, we show that this effect is not borne out experimentally for other carbons that should suffer this same compression. Thus we developed a robust alternative method for stereochemical assignment based on ^{1}H NMR coupling constants (31 examples) and supported by extensive DFT-based conformational analysis and calculation of [1]H-^{1}H coupling constants. DFT calculations of ^{13}C NMR chemical shifts also cast doubt upon the role of the "γ-gauche" effect on C1 and C3 chemical shifts in *trans*-THβCs.

Graphical Abstract

Are γ-gauche interactions in *trans*-tetrahydro-β-carbolines responsible for upfield ^{13}C NMR shifts (Δδ) of C1 and C3 relative to their *cis*-isomers?

pcarlier@vt.edu.

Conflicts of interest

There are no conflicts to declare.

Introduction

1,3-Disubsubstituted tetrahydro-β-carbolines (THβCs) **1** show a wide spectrum of biological activities,[1, 2] and serve as synthetic intermediates to the sarpagine/macroline/ajmaline class of natural products,[3] such as talcarpine **2** (Figure 1).[4] They are also prominent in medicinal chemistry as precursors to approved drugs and preclinical drug candidates: representative examples include the erectile dysfunction drug tadalafil (**3**)[5] and the anticancer candidate AZD9496 (**4**, currently in Phase I trials, Figure 1).[6] A compound of special interest for our group is **5a**, also known as MMV008138, which was originally identified[7] from a screen of a publicly available chemical library (the Malaria Box[8]). Although the configuration of **5a** was initially unknown, later studies[9–11] confirmed that **5a** is (1*R*,3*S*)-configured, and that it is a much more potent antimalarial agent than its *cis*-diastereomer **6a** (and enantiomers *ent*-**5a** and *ent*-**6a**). Compounds **5a** and **6a** were prepared by Pictet-Spengler reaction of (*S*)-Trp-OMe with 2,4-dichlorobenzaldehyde, followed by a separation of the diastereomeric esters **7a** and **8a**, and hydrolysis.[9] Ongoing optimization of this scaffold for antimalarial activity requires an accurate assignment of the relative stereochemistry of the ester precursors, and to this point we have used the ^{13}C NMR empirical rule of Ungemach et al.[12] In brief, C1 and C3 chemical shifts of *trans*-1,3- disubstituted THβCs (e.g., **5a**, **7a**) have been shown to be reliably upfield of those of the corresponding *cis*-diastereomers (e.g., **6a**, **8a**). The accuracy of this assignment method has been confirmed in several cases by X-ray crystallography[12–15] and NOESY/ROESY correlations (between H1 and H3 in *cis*-diastereomers),[13, 16–18] and appears to be secure. The ^{13}C NMR method is based on the so-called "γ-gauche effect," which attributes upfield shifts of carbons to steric compression resulting from gauche interaction with a γ-substituent.[19, 20] The γ-gauche effect of sp[3]-hybridized carbon has been well-documented in decalins,[21] norbornanes,[22] acetonides,[23] and conformationally-locked cyclohexanes.[24–26] It has also been invoked to deduce conformational preferences of conformationally-mobile substituted cyclohexanes,[27] and to deduce relative configuration of natural products[28] and various acyclic compounds.[29–32] However, in some cases the magnitude of this effect is very small.[22] In addition, for sp[2]-hybridized carbons, γ-gauche substituents can cause both small upfield[26] and small downfield[26, 27] shifts, and the effect on sp-hybridized carbons can also be very small.[24] As yet there is no firm consensus that the upfield shift of sp[3]-carbons possessing a γ-gauche interaction is actually steric in origin,[19, 33] and a number of observations in our laboratory (detailed below) did not comport with the steric hypothesis. Given these uncertainties, we validated a ^{1}H NMR coupling constant method, based on firm theoretical grounds, to reliably assign relative configuration in 1,3-disubstituted THβCs (31 examples). Reliance on ^{1}H NMR coupling constants rather than ^{13}C NMR chemical shifts confers several benefits, including reduced sample mass and experiment time requirements. Most significantly, unlike the ^{13}C NMR chemical shift method, this method can be applied reliably when only one diastereomer is in hand, as is the case for highly diastereoselective Pictet-Spengler reactions. [17, 34–36] Use of the ^{13}C NMR method in these cases requires further chemical transformation or subsequent synthesis of the other diastereomer. The assignment method presented herein is supported by an extensive density functional theory (DFT)-based conformational analysis and [1]H-^{1}H coupling constant prediction for two pairs of *trans*- and *cis*-diastereomers (**7a/8a**, **7b/8b**). Lastly, DFT calculations of ^{13}C chemical shifts of C1 and C3 in these four

compounds demonstrate that steric compression associated with the "γ-gauche" effect is *not* responsible for the upfield shift of C1 in *trans*-configured Pictet-Spengler adducts.

Results and Discussion

^{13}C and ^{1}H NMR Analysis of 1,3-disubstituted THβCs

For this study we analyzed the ^{1}H and ^{13}C NMR data of 30 additional pairs of diastereomeric THβC methyl esters related to **7a** and **8a**. Most of these compounds (**7b-z**, **8b-z**) were previously prepared by Pictet-Spengler reaction of (*S*)-Trp-OMe with the requisite benzaldehyde;[9, 37] five additional pairs of diastereomers derived from aliphatic aldehydes were also prepared for this work (**7aa-ae**, **8aa-ae**, Figure 2). Each pair of diastereomers was separated by column chromatography, and their configurations assigned as *cis*- or *trans*- using the ^{13}C NMR empirical rule[12] (See Table S1). Throughout our previous work, we noted that the *cis*-isomer was first-eluting in each case, as long as the eluent comprised a mixture of methylene chloride, hexane, and ethyl acetate. In the case of **7a** and **8a**, the assignment of *trans*-configuration to diastereomer **7a** was confirmed by X-ray crystallography of its methyl amide derivative.[9] It should be noted that the assignment of the C1 and C3 ^{13}C NMR peaks is not always straightforward: the C1 peak may be upfield or downfield of C3, depending on the substitution of the C1-aryl group. Furthermore, in the *trans*-isomers **7a**-**z**, the ^{13}C NMR chemical shifts of C3 and the methoxy carbon are often very close. Thus, the chemical shifts (^{1}H and ^{13}C) of **7a**, **8a**, and 15 other pairs of diastereomers were confirmed using HSQC, HMBC, and C-DEPT (See Tables S1–S4, Figures S1–S5). Taken together, over 31 pairs of diastereomers, the average C3 chemical shift is 52.5 ± 0.6 ppm for *trans*- and 56.8 ± 0.2 ppm for *cis*-, giving an average relative shift of −4.1 ± 0.6 ppm for C3 in **7a-ae** relative to **8a-ae** (C3 $\Delta\delta_{7-8}$, Table 1). Note that the C1 chemical shifts of the *trans*- and *cis*-esters **7a-ae** and **8a-ae** are significantly influenced by the 1-aryl and 1- alkyl substituents, as evidenced by the large standard deviations seen (51.7 ± 3.2 and 54.6 ± 3.4 ppm, for **7a-ae** and **8a-ae**, respectively). Nevertheless, within a pair of diastereomers, the relative shift of C1 in **7a-ae** relative to **8a-ae** is quite constant ($\Delta\delta_{7-8}$ = −2.9 ± 0.5 ppm). With this data in hand, the possible γ-gauche rationale for the upfield C1 and C3 chemical shifts in **7a-ae** relative to **8a-ae** ($\Delta\delta_{7-8}$, Table 1) can be evaluated. The tetrahydropyridine ring of *cis*-esters **8a-ae** should adopt an all pseudoequatorial conformation **A**, since the alternative half-chair conformation (not shown) would feature severe 1,3-diaxial interactions between C1' and CO_2Me (Figure 3). In contrast *trans*-esters **7a-ae** would likely populate two alternative half-chair conformations **B** and **C**, each featuring one pseudoequatorial (ψ_{eq}) and one pseudoaxial (ψ_{ax}) group.[38] As can be seen in the Newman projections in Figure 3 for the *cis*-isomers **8a-ae**, the CO_2Me group on C3 is anti to C1 (view down C3-N2 axis), and C1' of the C1-substituent is anti to C3 (view down N2-C1 axis). However, in conformer **B** (ψ_{eq}-CO_2Me) of **7a-ae**, C1' of the 1-substituent is gauche to C3, while CO_2Me remains anti to C1. Similarly, in conformer **C** (ψ_{ax}-CO_2Me) of **7a-ae**, the CO_2Me group is gauche to C1, while C1' remains anti to C3. Thus, if (and only if) both conformations **B** and **C** of **7a-ae** are populated, will both C1 and C3 of **7a-ae** experience steric compression relative to those carbons in **8a-ae**, and thus be shifted upfield in the ^{13}C NMR spectrum. Logically, such steric compression would also be expected to result in similar upfield ^{13}C NMR shifts for those carbons in **7a**-**ae** that interact with C1 and

C3 in this γ-gauche relationship, namely the CO_2Me C=O, and C1'. Interestingly however, this reciprocity is not seen. Over 31 pairs of compounds, the C=O ^{13}C NMR resonances of **7a-ae** are not upfield of those in **8a-ae**, but are in fact slightly downfield (δ_{7-8} = +0.8 ± 0.2 ppm, Table 1). Similarly, in the 16 cases of 1-aryl Pictet-Spengler adducts where we have unequivocally assigned C1', this resonance is not upfield in the *trans*- relative to the *cis*-isomer (Table 1, δ_{7-8} = +0.9 ± 0.5). These small downfield shifts of the CO_2Me C=O and aryl C1' carbons in **7aa-ae** might be ascribed to some not yet understood insensitivity of sp[2]-hybridized carbons to the γ-gauche effect. But in the five pairs of 1-alkyl Pictet-Spengler adducts, the sp[3]-hybridized C1' carbons are also not shifted upfield in **7aa-ae** relative to **8a-ae** (Table 1, δ_{7-8} = +0.7 ± 0.4). The failure of the gauche-oriented C1' and C3 sp[3]-carbons in **7aa-ae** (Figure 3B) to reciprocally exert upfield shifts on each other (relative to **8a-ae**) thus clearly undermines the proposal that "steric compression" determines C1 and C3 chemical shifts in THβCs.

With the rationale of the ^{13}C NMR chemical shift assignment method now uncertain, we looked for another method by which to reliably assign relative configuration. As mentioned earlier, NOESY/ROESY has been used periodically to confirm *cis*-configuration (correlation of H1 and H3),[13, 16–18] but we favored a method of greater operational simplicity. Two previous studies used the magnitude of vicinal coupling constants as a means of assigning *cis*- or *trans*-configuration, albeit for a single pair of diastereomers each.[13, 16] We sought to validate this method with the 31 additional pairs of diastereomers depicted in Figure 2. Inspection of conformer **A** for *cis*-esters **8a-ae** suggests that the three-bond coupling constants $^3J_{4\alpha-3}$ and $^3J_{4\beta-3}$ should be well differentiated: H4α is approximately gauche to H3, and H4β is approximately anti to H3 (Figure 3). In contrast, if the *trans*-diastereomers **7a-ae** populate both tetrahydropyridine conformations **B** and **C** as predicted, then $^3J_{4\beta-3}$ values will not be as well differentiated from the corresponding $^3J_{4\alpha-3}$ values, since H4β is approximately anti to H3 in conformer **B**, but is approximately gauche to H3 in conformer **C**. For **8a**, HSQC identified H4 resonances at 3.25 and 3.02 ppm. Individual irradiation of these two resonances resulted in 6.0% and ~0% NOE enhancement of H3 (3.99 ppm, Figure S5, Table S5), allowing assignment of H4α to the peak at 3.25 ppm, and H4β to the peak at 3.02 ppm. Based on these assignments we measured $^3J_{4\alpha-3}$ and $^3J_{4\beta-3}$ as 4.1 and 11.0 Hz, respectively. Thus, a large difference is seen in these coupling constants for **8a**, as expected. Similarly, we used 1D NOE experiments to assign H4β and H4α in *trans*-ester **7a** (Figure S4, Table S5). In this case the values of $^3J_{4\alpha-3}$ and $^3J_{4\beta-3}$ were much more similar (5.0 and 7.8 Hz, respectively). These findings are summarized in Figure 4. Based on the ^{1}H chemical shifts and ^3J values of **7a** and **8a**, H4α and H4β were assigned in the other 30 pairs of diastereomers, and the individual coupling constants were determined (Tables S3 & S4). Average ^{1}H chemical shifts and J values are shown in Table 2. As expected from their distance from the C1-substituent, the ^{1}H chemical shifts of H3, H4α, and H4β in **7a-ae** and **8a-ae** fall within very narrow ranges (Table 2, entries 1–3). As can be seen, the average value of $^3J_{4\beta-3}$ in *cis*-esters **8a-ae** is 11.1 ± 0.1 Hz (Table 2, entry 4), suggesting an approximately antiperiplanar arrangement of H4β and H3. In contrast, the average value of $^3J_{4\beta-3}$ in *trans*-esters **7a-ae** is consistently lower (7.3 ± 0.9 Hz), as expected if both conformers **B** and **C** were populated.[39] These well-differentiated average values of $^3J_{4\beta-3}$ for *cis*- and *trans*-diastereomers are very similar to those reported for the two

aforementioned pairs of diastereomers noted previously.[13, 16] Note that the average values of $^3J_{4\alpha-3}$ (entry 5) are similar for both **7a-ae** and **8a-ae**, consistent with a near gauche orientation of H4α and H3 in all three conformers **A**-**C**.

One noteworthy feature of the ^{1}H NMR spectra of **7a-ae** and **8a-ae** is the visible 5-bond coupling between H1 and H4α, and between H1 and H4β, as shown for **7b** and **8b** in Figure 5 (Table 2, entries 7–8). Note that for *trans*-1-aryl derivatives **7a-z**, H1 appears as a broad singlet, as shown for **7b** in Figure 5A. That the fine splitting in H4α and H4β is in fact due to 5-bond coupling to H1 was confirmed by single-frequency decoupling (Figure 5B). For *cis*-1-aryl derivatives **8a-z**, 5-bond coupling is occasionally seen at H1, as shown for **8b** in Figure 5C. Although 5-bond [1]H-^{1}H coupling is rare, it is particularly common in cyclohexenes,[40, 41] (which resemble the tetrahydropyridine ring of **7a-ae** and **8a-ae**) and has been noted at least once previously in Pictet-Spengler adducts.[13]

Density Functional Theory (DFT) Conformational Analysis of 7a/8a and 7b/8b

As described above, values of $^3J_{4\beta-3}$ effectively distinguish *trans*-esters **7a-ae** from *cis*-esters **8a-ae**. Furthermore, the observed values of $^3J_{4\beta-3}$ in these compounds appear reasonable based on a first-principles conformational analysis (Figure 3). To further substantiate our method for stereochemical assignment we undertook computational studies of the possible conformers of **7a**/**8a** and **7b**/**8b**. Multiple automated conformer searches were performed at the MMFF94 level, starting from at least two initial geometries of each compound. These structures were then optimized at B3LYP/6–31G(d)[42, 43] to give 16 conformers of **7a**, 14 conformers of **8a**, and 8 conformers each for **7b** and **8b**. As shown in Table 3, these conformers can be classified with respect to four structural features, and thus grouped into eight ensembles of conformers.

First, the approximate half-chair conformation of the tetrahydropyridine ring can be classified as having a ψ_{ax}- or ψ_{eq}-CO_2Me group; representative calculated structures of **7a** exhibiting these features are shown in Figure 6 (**I** and **II**, respectively). Interestingly, the orientation of the 1-aryl groups in **7a** and **7b** does not differ significantly among these different tetrahydropyridine conformers. For **7a**, the C1'-C1-C9a-N9 dihedral angle φ for **II** (66.8°) is only slightly larger than that seen in **I** and **III** (52.7 and 46.1°, respectively), despite the expectation that the 1-aryl group would be pseudoaxial in **II** and pseudoequatorial in **I** and **III**. The larger than expected φ value in **I** and **III** is likely a consequence of allylic strain of the 1-aryl group and N9. Second, the 2'-Cl of **7a** and **8a** can be oriented *exo*- or *endo*- to the tetrahydropyridine ring: see Figure 6 for calculated structures **I/II** (*exo*-) vs **III** (*endo*-). Note that this isomerism is absent in **7b** and **8b**, which feature an unsubstituted phenyl ring. Third, the N-H can be axial or equatorial, and fourth, the CO_2Me group can be hydrogen- bound to the NH, or not hydrogen-bound.[44] These last two features are illustrated in the representative computed structures of **7a** in Figure 6. In *trans*-ester **7a**, eight ψ_{ax}-CO_2Me and eight ψ_{eq}-CO_2Me conformations were located (cf. **B** and **C**, Figure 3). In the *cis*-isomer **8a**, only six ψ_{ax}-CO_2Me conformers and eight ψ_{eq}-CO_2Me conformations were found. As expected, the six ψ_{ax}-CO_2Me conformers of **8a** are all much higher in energy than the ψ_{eq}-CO_2Me conformations, due to 1,3-di-pseudoaxial interaction of the C3-CO_2Me and C1-aryl groups.[45] As depicted in Figure 6, for **7a** and **8a**,

the 2'-Cl group can adopt an *exo-* or *endo-*orientation with respect to the tetrahydropyridine ring. This type of conformational isomerism is not observed in **7b/8b**, since they bear an unsubstituted phenyl ring; thus, the number of possible conformations available to **7a/8a** is generally double that of **7b/8b**. The axial and equatorial orientations of the hydrogen (H2) are roughly equally represented among the conformers. In conformations featuring a ψ_{eq}-CO_2Me group, both *ax*-H2 and *eq*-H2 can hydrogen-bond to the CO_2Me group, via the C=O or OMe oxygen atoms. In contrast, for conformations featuring a ψ_{ax}-CO_2Me group, only *eq*-H2 can form an intramolecular H-bond via the C=O or OMe oxygen atoms. In ψ_{ax}-CO_2Me/*ax*-H2 conformations, an intramolecular H-bond is geometrically impossible (e.g. structure **III**, Figure 6). Structures of the lowest energy conformers of **7a**, **8a**, **7b**, and **8b** are presented in the Supporting Information (Figures S6 & S7). To calculate free energies of these conformers at 298 K, single point energies were calculated using the mPW1PW91[47]and B3LYP functionals, at a larger basis set (6–311+G(2d,p)), and with PCM[48] implicit solvation ($CHCl_3$). As described below, the 6–311+G(2d,p) basis set, mPW1PW91 functional, and PCM solvation model were chosen based on their suitability for ^{13}C NMR shift calculations.[49] In addition, we also calculated single point energies at M06–2X/def2-TZVP (with PCM solvation), since the M06–2X functional[50, 51] has been recommended for accurate energies of conformers, especially in conjunction with the def2-TZVP basis set.[52, 53] Free energy corrections (based on B3LYP/6–31G(d) frequencies) were then applied to these single point energies (Tables S6–S13).

Boltzmann distributions of the conformers of **7a/8a**, **7b/8b** calculated using mPW1PW91/6–311+G(2d,p) (PCM, $CHCl_3$) free energies were very similar to those based on B3LYP/6–311+G(2d,p) (PCM, $CHCl_3$) free energies (Table S14). M06–2X/def2-TZVP (PCM, $CHCl_3$) free energy-based Boltzmann distributions largely follow these trends, but for **8a** and **8b** show a diminished preference for conformers in the ψ_{eq}-CO_2Me ensemble (e.g. **A**, Figure 3) vs those in the ψ_{ax}-CO_2Me ensemble (see Table S14). As a consequence (see below), mPW1PW91 and B3LYP/6–311+G(2d,p)-based Boltzmann distributions give superior prediction of $^3J_{4\beta-3}$, relative to those based on M06–2X/def2-TZVP. Furthermore since calculations at mPW1PW91/6–311+G(2d,p) give improved prediction of ^{13}C NMR chemical shifts relative to those based on B3LYP/6–311+G(2d,p), (see below), for simplicity we will base all calculations below on mPW1PW91/6–311+G(2d,p) (PCM, $CHCl_3$) Boltzmann weights of the conformers. These values were summed to calculate the percentage occupying each of the four pairs of conformational ensembles noted previously (Table 4).

As anticipated, *trans*-esters **7a** and **7b** significantly populate both the ψ_{ax}-CO_2Me and ψ_{eq}-CO_2Me conformational ensembles (cf. **B** and **C**, Figure 3). For **7a**, the lowest energy ψ_{ax}-CO_2Me conformation (**7a**-01) is only 0.9 kcal/mol higher in energy than global minimum ψ_{eq}-CO_2Me structure (**7a**-08, Table S7, Figure S6). For **7b**, the lowest energy ψ_{ax}-CO_2Me conformation (**7b**-01) and lowest energy ψ_{eq}-CO_2Me conformation (**7b**-05) are within 0.02 kcal/mol of each other (Table S9, Figure S7). In contrast, *cis*-esters **8a** and **8b** adopt >97% and >99% ψ_{eq}-CO_2Me conformations respectively.[54] For **8a** and **8b**, the lowest energy ψ_{ax}-CO_2Me conformations are 3.1 (**8a**-04) and 4.6 kcal/mol (**8b**-05) higher in energy than global minimum ψ_{eq}-CO_2Me structures (**8a**-01 and **8b**-03, Figures S6 & S7, Tables S11 & S13).

As discussed at the outset, ψ_{ax}-CO_2Me conformations of **8a** and **8b** would be unstable by virtue of 1,3-dipseudoaxial interactions with the ψ_{ax}-aryl group at C1. Thus, these DFT calculations support the first-principles conformational analysis presented in Figure 3, and the values of $^3J_{4\beta-3}$ reported in Table 2. Other noteworthy features of our calculations are: 1) in **7a** and **8a** there is a significant preference for the *exo*-2'-Cl orientation, which appears to be steric in origin; 2) *ax*-H2 and *eq*-H2 conformations are similar in energy for all four compounds; 3) intramolecularly H-bonded structures are much more favorable than non-H-bonded structures for all four compounds.

DFT calculations of select ^{1}H-^{1}H coupling constants in 7a/8a and 7b/8b

Using mPW1PW91/6–311+G(2d,p) (PCM, CHCl$_3$) Boltzmann weights we then calculated select ^{1}H-^{1}H coupling constants at B3LYP/6–31G(d,p)u+1s//B3LYP/6–31G(d), which has been found to be economical and accurate (RMSD < 0.5 Hz) for a wide range of organic molecules.[56] As can be seen in Table 5, this method worked very well for **7a**/**8a** and **7b**/**8b**. For the 5 coupling constants previously presented in Table 2, over 4 compounds, excellent accuracy (RMSD < 0.4 Hz, Tables S15,16) was obtained. Most importantly, the close correspondence of calculated and observed values of $^3J_{4\beta-3}$ and $^3J_{4\alpha-3}$ suggests that the mPW1PW91/6–311+G(2d,p) (PCM, CHCl$_3$) Boltzmann weights accurately capture the distribution of ψ_{ax}-CO_2Me and ψ_{ax}-CO_2Me conformers of the tetrahydropyridine ring in **7a**/**8a** and **7b**/**8b**. For reference, use of the M06–2X/def2-TZVP Boltzmann distributions in these calculations gave less accurate values of $^3J_{4\beta-3}$ for **8a** and **8b** (8.8 and 10.2 Hz, respectively, Table S16) as a consequence of the diminished energetic difference between the ψ_{ax}-CO_2Me and ψ_{ax}-CO_2Me conformers.

DFT calculations of ^{13}C chemical shifts of 7a/8a and 7b/8b

With the B3LYP/6–31G(d) geometries and mPW1PW91/6–311+G(2d,p) (PCM, CHCl$_3$) Boltzmann distribution of the conformers of **7a**/**8a** and **7b**/**8b** validated by the calculated ^{1}H-^{1}H coupling constants in Table 5, we were positioned to determine whether the distinctive C1 and C3 chemical shifts of the *cis*- and *trans*-diastereomers could be reproduced by computation. We thus calculated ^{13}C NMR chemical shifts (δ) for each conformer of **7a**, **7b**, **8a**, and **8b** from the B3LYP/6–31G(d) geometries at the B3LYP/6–311+G(2d,p) (PCM, CHCl$_3$) and mPW1PW91/6–311+G(2d,p) (PCM, CHCl$_3$) levels of theory (Table S17–S20). These functionals, basis set, and solvation model were selected based on their excellent performance in a recent study of colchicine.[49] The weighted average ^{13}C NMR chemical shifts of each carbon in **7a**, **7b**, **8a**, and **8b** were then calculated using the calculated Boltzmann populations; mean average deviations (MAD) of the calculated chemical shifts from the observed values were calculated to assess the performance of each functional. As seen in Table 6, both functionals predict ^{13}C NMR chemical shifts well, giving MAD of ~2 ppm or less. The slightly smaller MAD values seen for **7b**/**8b** relative to **7a**/**8a** is a consequence of inaccurate calculation of the ^{13}C chemical shifts for Cl-bearing carbons C2' and C4' in **7a** and **8a** (see Tables S17, S19). However, over the four compounds examined, the mPW1PW91 functional performs better than the B3LYP functional (average MAD = 1.4 ppm vs 1.8 ppm). A recent study of the calculated ^{13}C NMR spectrum of colchicine in CDCl$_3$ also noted improved accuracy of the mPW1PW91 functional relative to

B3LYP, and our calculated MAD (1.4 ppm) is even lower than they reported (1.9 ppm).[49] As can be seen in Table 7, ^{13}C NMR chemical shifts for C3, C1, C=O, and C1' calculated by this method very closely match the observed values (italics) for all four compounds, with deviations generally less than 2 ppm. Looking at the difference in chemical shift for a particular carbon between diastereomers (δ_{7-8}), the congruity is even better. For example, the C1 and C3 δ_{7-8} values for **7a/8a** are predicted to be –4.1 and –2.9 ppm; the observed δ_{7-8} values are –4.4 and –2.6 ppm, respectively; the correspondences for **7b/8b** are also very close. Note that this DFT method also recapitulates the observed slight (+0.5 to +1.3 ppm) downfield shifts of C=O and C1' in the *trans*-isomers. These close correspondences are also seen using the B3LYP functional (Table S17–S20). Thus, DFT predicts the observed upfield shifts of C1 and C3 in **7a-b** relative to **8a-b**, as well as the slight downfield shifts of C=O and C1'.

Computational evaluation of the role of steric compression in the ^{13}C chemical shifts of C1 and C3 in 7a and 7b

With the accuracy of DFT-derived ^{13}C NMR chemical shifts for **7a/8a** and **7b/8b** now established, we are in a position to ask whether these upfield shifts of C1 and C3 in **7a** and **7b** relative to **8a** and **8b** can be attributed to "steric compression." *If so, the chemical shifts of C1 and C3 in **7a** and **7b** should be dependent on the conformation of the tetrahydropyridine ring.* By grouping the individual conformers of **7a** and **7b** into two overall ψ_{eq}- and ψ_{ax}-CO$_2$Me tetrahydropyridine conformational ensembles (i.e. **B** and **C**, Figure 3), and recalculating the weighted average ^{13}C NMR chemical shifts at C1 and C3, we can assess the effect of γ-gauche-associated steric compression (Figure 7, Tables S19-S20). As can be seen, the calculated ^{13}C chemical shifts of C3 in **7a** and **7b** in ensemble **B** are considerably upfield of the values in ensemble **C** (C3 δ_{B-C} = –5.2 and –5.0 ppm respectively). These calculated upfield shifts could be consistent with steric compression of C3 resulting from γ-gauche interaction with the C1-aryl group in ensemble **B** (cf. Figure 3). However, no significant differences are seen in the chemical shifts of C1 in **7a** and **7b** between ensembles **B** and **C** (C1 δ_{B-C} = –0.3 and +0.6 ppm, respectively), despite its γ-gauche orientation to the ψ_{ax}-C3-CO$_2$Me group in ensemble **C**. These observations are replicated at the B3LYP/6–311+G(2d,p) (PCM, CHCl$_3$)//B3LYP/6–31G(d) level (Tabled S22–S22). Thus, the uniform upfield shift of C1 in **7a-ae** relative to **8a-ae** (Table 1) cannot be attributed to the γ-gauche effect, since the C1 chemical shifts remain unchanged whether the C1-CO$_2$Me group is gauche (ensemble **C**) or anti- (ensemble **B**).

Conclusions

In this report we have demonstrated that the *trans*- or *cis*-configuration of 1,3-disubstituted THβCs can be reliably assigned by ^{1}H NMR spectroscopy, based on a particular coupling constant ($^3J_{4\beta-3}$). Over 31 *cis*-esters compounds **8a-ae**, the value of $^3J_{4\beta-3}$ is 11.1 ± 0.1 Hz, indicating they exclusively populate a tetrahydropyridine conformational ensemble that features a ψ_{eq}-CO$_2$Me group at C3 (**A**, Figure 3). In contrast for the 31 *trans*-esters compounds **7a-ae**, the value of $^3J_{4\beta-3}$ is 7.3 ± 1.2 Hz, indicating these compounds populate two nearly equienergetic tetrahydropyridine conformational ensembles: one featuring a ψ_{eq}-CO$_2$Me group at C3 (**B**, Figure 3), and one featuring a ψ_{ax}-CO$_2$Me group at C3 (**C**, Figure

3). In every case these assignments match those made by the ^{13}C NMR chemical shift method of Ungemach et al,[12] but this ^{1}H NMR assignment method has several benefits. In addition to reduced sample quantity and experiment time requirements, it can be applied when only one stereoisomer is in hand. Extensive DFT calculations support the conformational analysis undergirding the ^{1}H NMR assignment method, including accurate (RMSD = 0.4 Hz) calculation of $^3J_{4\beta-3}$ and other ^{1}H-^{1}H coupling constants. Furthermore, these calculations show that the presence or absence of a γ-gauche substituent has no effect on the ^{13}C NMR chemical shift of C1 in **7a** and **7b** (Figure 7). This calculated result, combined with the observed failure of C1 and C3 to exert reciprocal upfield shifts of the C=O and C1' carbons in **7a**-**ae** (Table 1), thus challenge the conceptual foundation of the traditional ^{13}C NMR chemical shift assignment method for 1,3-disubstituted THβCs. With this foundation in doubt, one cannot predict scenarios under which the method would fail to properly assign *trans*- and *cis*-THBCs. Since biological activity within the medicinally important 1,3-disubstituted-THβC scaffold is typically very sensitive to configuration, [2, 5, 9, 37] a missed assignment could muddy emerging structure-activity relationships and mislead investigators. In contrast, the sound theoretical foundation of the $^3J_{4\beta-3}$ assignment method described herein allows one to use standard tools of conformational analysis to anticipate conditions under which it might fail. This important feature and the other advantages listed above commend its use to synthetic and medicinal chemists.

Methods

Computational

To extensively probe the conformational space available to compounds **7a**, **7b**, **8a**, and **8b**, automated conformer searches (MMFF94) were performed using Spartan '16,[57] starting from at least two different geometries. These MMFF94 minima were then optimized at B3LYP/6–31G(d) using Gaussian 09,[58] giving the numbers of conformers listed above in Table 4. In each case vibrational frequency analysis (NIMAG=0) confirmed that each stationary point was a minimum. Individual conformers of **7a**, **7b**, **8a**, and **8b** are identified in the Supporting Information as **7a**-01 to **7a**-16, **7b**-01 to **7b**-08, **8a**-01 to **8a**-14, **8b**-01 to **8b**-08, respectively. Single point energies of each conformer were calculated with three different functionals and larger basis sets, as described above: B3LYP/6–311+G(2d,p), mPW1PW91/6–311+G(2d,p) and M06–2X/def2-TZVP each with implicit solvation SCRF=(PCM,Solvent=Chloroform). Free energies were calculated by adding the free energy (298 K) corrections derived from unscaled B3LYP/6–31G(d) frequencies to these single point energies, to derive the corresponding Boltzmann distributions. The overall population of each of the eight conformational ensembles described in Table 4 (and Table S14) were calculated by summing the Boltzmann populations of the appropriate individual conformers.

Calculated J_{HH} coupling constants shown in Table 5 were obtained using the B3LYP functional with core-augmented 6–31G(d,p) basis set ("6–31G(d,p)u+1s"). Note that only Fermi contact terms were evaluated, and only couplings between the hydrogen atoms of interest (H4β, H4α, H3, H1) were specified for calculation. This approach was selected based on its high accuracy (RMSD <0.5 Hz over a large test set) and low computational cost. [56] Interestingly, although ^{1}H chemical shift modeling benefits from inclusion of implicit

solvation, this study demonstrated that implicit solvation does not improve the accuracy of calculated J_{HH} values;[56] thus we calculated values in the gas phase. The coupling constants ($^3J_{4\beta-3}$, $^3J_{4\alpha-3}$, $^2J_{4\beta-4\alpha}$, $^5J_{4\beta-1}$, $^5J_{4\alpha-1}$) in each conformer of **7a**, **8a**, **7b**, and **8b**, (scaled by the recommend factor of 0.9117) are given in Table S15, which includes a sample Gaussian route section to perform these calculations. To obtain weighted average J_{HH} coupling constants, the various Boltzmann distributions were applied (Table 5 and S16).

Shielding tensors σ for each carbon in each conformer were calculated from the B3LYP/6–31G(d) geometries at the B3LYP/6–311+G(2d,p) (PCM, CHCl$_3$) and mPW1PW91/6–311+G(2d,p) (PCM, CHCl$_3$) levels of theory. These functionals, basis set, and solvation model were selected based on their excellent performance in a recent study of the ^{1}H and ^{13}C NMR solution spectra of colchicine.[49] The corresponding ^{13}C NMR chemical shifts were calculated according to the formula δ = (σ − b)/a, where a = slope and b = intercept.[59] The values of a and b were taken from the aforementioned study of colchicine,[49] and were a = −1.043 , b = 181.717 for B3LYP/6–311+G(2d,p) (PCM=CHCl$_3$), and a = −1.042, b = 186.357 for mPW1PW91/6–311+G(2d,p) (PCM=CHCl$_3$). The weighted average ^{13}C chemical shifts of each carbon were then determined using the calculated Boltzmann distributions, and compared to experimental chemical shifts to obtain the MAD for each compound studied.

Chemistry

All NMR spectra were acquired in CDCl$_3$. As described above, 1-aryl-substituted Pictet-Spengler adducts **7a-z** and **8a-z** were prepared previously;[9, 37] ^{1}H and ^{13}C NMR analyses described in this paper were performed on archived samples.

Experimental

Synthesis of 7aa and 8aa

To a mixture of **L**-tryptophan methyl ester hydrochloride (514 mg, 2.02 mmol), 4Å molecular sieves (1 g, powdered), and pentanal (0.24 mL, 2.26 mmol), CH$_2$Cl$_2$ (6 mL) was added under nitrogen. The resulting mixture was stirred at room temperature for 48 hours. TFA (0.3 mL, 3.92 mmol) was added dropwise. Reaction mixture was further stirred at room temperature for additional 24 hours. Reaction was cooled to 0 °C and saturated aqueous solution of NaHCO$_3$ (6 mL) was added, followed by addition of EtOAc (6 mL). After stirring for 30 min at 0 °C, the molecular sieves were filtered and phases of the filtrate were partitioned and the aqueous layer was extracted with EtOAc (3 × 10 mL). The combined organic layers were washed with saturated aqueous NaCl solution (25 mL), dried over Na$_2$SO$_4$ and concentrated in vacuo. Compounds **7aa** and **8aa** were separated from the crude material by flash chromatography (gradient, from 1:1 CH$_2$Cl$_2$: hexane to 2:2:1 CH$_2$Cl$_2$: hexane : EtOAc) to give **8aa** (190 mg, 33%, first-eluting, off-white solid) and **7aa** (45 mg, 8%, second-eluting, yellow oil). A mixed fraction of **7aa** and **8aa** (162 mg, 28% yield) was also obtained.

Methyl (1*R*,3*S*)-1-butyl-2,3,4,9-tetrahydro-1*H*-pyrido[3,4-*b*]indole-3-carboxylate (7aa): ^{1}H NMR (400 MHz, CDCl$_3$) δ 7.73 (s, 1H), 7.49 (ddd, *J* = 7.6, 1.4, 0.7 Hz, 1H),

7.31 (ddd, *J* = 8.0, 1.2, 0.7 Hz, 1H), 7.15 (ddd, *J* = 8.0, 7.1, 1.4 Hz, 1H), 7.10 (ddd, *J* = 7.6, 7.1, 1.1 Hz, 1H), 4.24 (dd, *J* = 8.3, 4.9 Hz, 1H), 3.99 (dd, *J* = 7.3, 5.3 Hz, 1H), 3.75 (s, 3H), 3.12 (ddd, *J* = 15.3, 5.3, 1.2 Hz, 1H), 2.99 (ddd, *J* = 15.3, 7.3, 1.5 Hz, 1H), 1.93 (s, 1H), 1.84 – 1.68 (m, 2H), 1.58 – 1.44 (m, 2H), 1.43 – 1.35 (m, 2H), 0.94 (t, *J* = 7.2 Hz, 3H). ^{13}C NMR (101 MHz, CDCl$_3$) δ 174.4, 136.0, 135.8, 127.2, 121.7, 119.5, 118.1, 110.8, 107.0, 52.7, 52.2, 50.4, 35.5, 28.5, 25.1, 22.9, 14.2. This compound has been reported previously without full NMR characterization.[60]

Methyl (1*S*,3*S*)-1-butyl-2,3,4,9-tetrahydro-1*H*-pyrido[3,4-*b*]indole-3-carboxylate (8aa): ^{1}H NMR (400 MHz, CDCl$_3$) δ 7.79 (s, 1H), 7.48 (d, *J* = 7.7 Hz, 1H), 7.36 – 7.30 (m, 1H), 7.16 (td, *J* = 8.1, 7.6, 1.3 Hz, 1H), 7.11 (ddd, *J* = 7.6, 7.2, 1.2 Hz, 1H), 4.20 (ddt, *J* = 8.3, 4.1, 2.2 Hz, 1H), 3.83 (s, 3H), 3.80 (dd, *J* = 11.2, 4.2 Hz, 1H), 3.13 (ddd, *J* = 15.1, 4.2, 1.9 Hz, 1H), 2.82 (ddd, *J* = 15.1, 11.2, 2.6 Hz, 1H), 2.00 – 1.91 (m, 1H), 1.72 (dddd, *J* = 13.8, 10.5, 8.1, 5.2 Hz, 1H), 1.52 – 1.44 (m, 2H), 1.39 (dddd, *J* = 14.2, 8.7, 6.9, 5.4 Hz, 2H), 0.94 (t, *J* = 7.1 Hz, 3H). ^{13}C NMR (101 MHz, CDCl$_3$) δ 173.9, 136.0, 135.8, 127.3, 121.8, 119.7, 118.1, 110.9, 108.2, 56.6, 52.9, 52.3, 34.7, 27.6, 26.1, 23.1, 14.1. This compound has been reported previously without full NMR characterization.[60]

Synthesis of 7ab and 8ab

The procedure for **7aa**/**7ab** above was followed using **L**-tryptophan methyl ester hydrochloride (1.281 mg, 5.03 mmol), 4Å molecular sieves (3.5 g, powdered), and cyclohexanecarboxaldehyde (0.58 mL, 5.09 mmol). Following workup, **7ab** and **8ab** were isolated by column chromatography (5:5:3.5 CH$_2$Cl$_2$: hexane: EtOAc) to give **8ab** (1.02 g, 65%, first-eluting, pale yellow solid) and **7ab** (149 mg, 10% yield, second-eluting, off-white solid). A mixed fraction of **7ab** and **8ab** (190 mg, 12% yield) was also obtained.

Methyl (1*R*,3*S*)-1-cyclohexyl-2,3,4,9-tetrahydro-1*H*-pyrido[3,4-*b*]indole-3-carboxylate (7ab): ^{1}H NMR (400 MHz, CDCl$_3$) δ 7.76 (s, 1H), 7.49 (ddt, *J* = 7.6, 1.5, 0.8 Hz, 1H), 7.31 (dt, *J* = 8.0, 1.0 Hz, 1H), 7.18 – 7.07 (m, 2H), 4.08 (d, *J* = 5.2 Hz, 1H), 4.02 (dd, *J* = 6.9, 5.3 Hz, 1H), 3.72 (s, 3H), 3.10 (ddd, *J* = 15.3, 5.3, 1.3 Hz, 1H), 3.00 (ddd, *J* = 15.3, 6.9, 1.5 Hz, 1H), 1.87 – 1.78 (m, 4H), 1.76 – 1.65 (m, 4H), 1.37 – 1.10 (m, 6H). ^{13}C NMR (101 MHz, CDCl$_3$) δ 174.7, 135.9, 134.6, 127.2, 121.7, 119.5, 118.1, 110.8, 107.9, 55.4, 53.5, 52.2, 43.3, 30.4, 28.6, 26.7, 26.5, 26.5, 25.0. mp 150.2–154.8 °C. This compound has been previously reported and both NMR and mp data are consistent with the literature.[61, 62]

Methyl (1*S*,3*S*)-1-cyclohexyl-2,3,4,9-tetrahydro-1*H*-pyrido[3,4-*b*]indole-3-carboxylate (8ab): ^{1}H NMR (400 MHz, CDCl$_3$) δ 7.80 (s, 1H), 7.48 (ddd, *J* = 7.6, 1.4, 0.7 Hz, 1H), 7.34 (dt, *J* = 8.0, 1.0 Hz, 1H), 7.19 – 7.08 (m, 2H), 4.16 (q, *J* = 2.3 Hz, 1H), 3.82 (s, 3H), 3.74 (dd, *J* = 11.2, 4.1 Hz, 1H), 3.11 (ddd, *J* = 14.9, 4.1, 1.8 Hz, 1H), 2.78 (ddd, *J* = 14.9, 11.2, 2.6 Hz, 1H), 1.89 – 1.68 (m, 6H), 1.51 – 1.17 (m, 6H). ^{13}C NMR (101 MHz, CDCl$_3$) δ 174.0, 136.1, 134.9, 127.4, 121.7, 119.6, 118.0, 110.9, 109.3, 57.8, 56.6, 52.3, 42.5, 29.8, 27.0, 27.0, 26.7, 26.5, 26.1. mp 132.3–135.3 °C. This compound has been previously reported and both NMR and mp data are consistent with literature.[61, 62]

Synthesis of 7ac and 8ac

The procedure for **7aa**/**8aa** above was followed using **L**-tryptophan methyl ester hydrochloride (501 mg, 1.97 mmol) and 2-ethylbutanal (0.27 mL, 2.19 mmol). Purification on column chromatography (5:5:2 CH_2Cl_2: hexane: EtOAc) yielded **8ac** (166.4 mg, 28%, first-eluting, yellow glass) and **7ac** (34.3 mg, 6%, second-eluting, yellow oil). A mixed fraction of **7ac** and **8ac** (312.3 mg, 52.8% yield) was also obtained.

Methyl (1*R*,3*S*)-1-(pentan-3-yl)-2,3,4,9-tetrahydro-1*H*-pyrido[3,4-*b*]indole-3-carboxylate (7ac): ^{1}H NMR (400 MHz, CDCl$_3$) δ 7.74 (s, 1H), 7.49 (ddt, *J* = 7.5, 1.5, 0.8 Hz, 1H), 7.31 (dt, *J* = 7.8, 1.1 Hz, 1H), 7.17 – 7.12 (m, 1H), 7.10 (td, *J* = 7.4, 1.2 Hz, 1H), 4.48 (dt, *J* = 3.3, 1.8 Hz, 1H), 4.05 (t, *J* = 5.2 Hz, 1H), 3.68 (s, 3H), 3.12 (dt, *J* = 5.4, 1.7 Hz, 2H), 1.91 (s, 2H), 1.63 – 1.48 (m, 3H), 1.38 – 1.23 (m, 3H), 1.05 (t, *J* = 7.2 Hz, 3H), 0.84 (t, *J* = 7.5 Hz, 3H). ^{13}C NMR (101 MHz, CDCl$_3$) δ 174.7, 136.0, 134.7, 127.4, 121.6, 119.4, 118.0, 110.8, 108.2, 54.1, 52.2, 51.0, 46.7, 24.4, 23.1, 22.7, 12.6, 12.3. HRMS (ESI) [M+H][+] calculated for $C_{18}H_{24}N_2O_2$: 301.1911. Found: 301.1910.

Methyl (1*S*,3*S*)-1-(pentan-3-yl)-2,3,4,9-tetrahydro-1*H*-pyrido[3,4-*b*]indole-3-carboxylate (8ac): ^{1}H NMR (400 MHz, CDCl$_3$) δ 7.76 (s, 1H), 7.48 (ddt, *J* = 7.7, 1.5, 0.7 Hz, 1H), 7.33 (ddd, *J* = 8.0, 1.2, 0.8 Hz, 1H), 7.18 – 7.13 (m, 1H), 7.11 (ddd, *J* = 7.6, 7.1, 1.2 Hz, 1H), 4.35 (q, *J* = 2.3 Hz, 1H), 3.82 (s, 3H), 3.74 (dd, *J* = 11.2, 4.1 Hz, 1H), 3.12 (ddd, *J* = 15.0, 4.1, 1.9 Hz, 1H), 2.78 (ddd, *J* = 15.0, 11.2, 2.6 Hz, 1H), 1.69 (s, 1H), 1.63 – 1.53 (m, 3H), 1.37 – 1.24 (m, 2H), 1.04 (t, *J* = 7.3 Hz, 3H), 0.89 (t, *J* = 7.5 Hz, 3H). ^{13}C NMR (101 MHz, CDCl$_3$) δ 174.1, 136.0, 135.5, 127.5, 121.7, 119.6, 117.9, 110.9, 109.5, 56.6, 54.6, 52.3, 46.1, 26.2, 23.3, 22.8, 13.2, 12.8. HRMS (ESI) [M+H][+] calculated for $C_{18}H_{24}N_2O_2$: 301.1911. Found: 301.1908

Synthesis of 7ad and 8ad

The procedure for **7aa**/**8aa** above was followed using **L**-tryptophan methyl ester hydrochloride (514 mg, 2.02 mmol) and trimethylacetaldehyde (0.65 mL, 5.98 mmol). Purification on column chromatography (5:5:2 CH_2Cl_2: hexane: EtOAc) yielded **8ad** (1.9 mg, 0.3%, first-eluting, yellow oil) a mixed fraction of **7ad** and **8ad** (289.7 mg, 50%, yellow oil). Recrystallization of the mixture from EtOAc gave a small quantity of pure **7ad** (17.1 mg, 3%, colorless crystals).

Methyl (1*R*,3*S*)-1-(*tert*-butyl)-2,3,4,9-tetrahydro-1*H*-pyrido[3,4-*b*]indole-3-carboxylate (7ad): ^{1}H NMR (400 MHz, CDCl$_3$) δ 7.78 (s, 1H), 7.50 (ddt, *J* = 7.7, 1.5, 0.8 Hz, 1H), 7.35 – 7.28 (m, 1H), 7.18 – 7.13 (m, 1H), 7.10 (ddd, *J* = 7.7, 7.1, 1.2 Hz, 1H), 4.09 (app. t, *J* = 5.2 Hz, 1H), 4.07 (t, *J* = 1.4 Hz, 1H), 3.63 (s, 3H), 3.11 (ddd, *J* = 15.0, 5.1, 1.5 Hz, 1H), 3.08 (ddd, *J* = 15.0, 5.3, 1.6 Hz, 1H), 1.08 (s, 9H). ^{13}C NMR (126 MHz, CDCl$_3$) δ 175.1, 135.9, 133.7, 127.0, 121.8, 119.4, 118.1, 110.7, 109.2, 59.4, 54.4, 52.1, 36.8, 27.3, 24.7. HRMS (ESI) [M+H][+] calculated for $C_{17}H_{22}N_2O_2$: 287.1754. Found: 287.1753. mp = 141.3–142.4 °C

Methyl (1*S*,3*S*)-1-(*tert*-butyl)-2,3,4,9-tetrahydro-1*H*-pyrido[3,4-*b*]indole-3-carboxylate (8ad): ^{1}H NMR (400 MHz, CDCl$_3$) δ 7.90 (s, 1H), 7.50 (d, *J* = 8.1 Hz, 1H),

7.33 (dt, J = 8.1, 0.9 Hz, 1H), 7.17 (ddd, J = 8.1, 7.1, 1.3 Hz, 1H), 7.11 (ddd, J = 8.1, 7.1, 1.1 Hz, 1H), 4.03 (s, 1H), 3.83 (s, 3H), 3.68 (dd, J = 11.2, 3.6 Hz, 1H), 3.14 (ddd, J = 14.6, 3.6, 1.5 Hz, 1H), 2.77 (ddd, J = 14.6, 11.2, 2.4 Hz, 1H), 1.13 (s, 9H). ^{13}C NMR (101 MHz, CDCl$_3$) δ 174.0, 136.0, 134.6, 126.9, 121.9, 119.6, 118.0, 110.8, 62.6, 56.5, 52.3, 35.7, 27.1, 26.4. This compound has been previously reported and NMR data are consistent with literature.[63]

Synthesis of 7ae and 8ae

The procedure for **7aa**/**8aa** above was followed using **L**-tryptophan methyl ester hydrochloride (502 mg, 1.97 mmol) and 3-methylbutanal (0.23 mL, 2.14 mmol). Purification on column chromatography (5:5:2 CH$_2$Cl$_2$: hexane: EtOAc) to give **8ae** (152.8 mg, 27%, first-eluting, yellow oil) and **7ae** (117.4 mg, 21% yield, second-eluting, yellow oil). A mixed fraction of **7ae** and **8ae** (225.6 mg, 40% yield) was also obtained.

Methyl (1*R*,3*S*)-1-isobutyl-2,3,4,9-tetrahydro-1*H*-pyrido[3,4-*b*]indole-3-carboxylate (7ae): ^{1}H NMR (400 MHz, CDCl$_3$) δ 7.74 (s, 1H), 7.48 (ddt, J = 7.7, 1.5, 0.8 Hz, 1H), 7.30 (ddd, J = 8.0, 1.2, 0.8 Hz, 1H), 7.15 (ddd, J = 8.0, 7.1, 1.4 Hz, 1H), 7.10 (ddd, J = 7.6, 7.1, 1.2 Hz, 1H), 4.32 (dd, J = 10.0, 4.2 Hz, 1H), 3.99 (dd, J = 7.4, 5.3 Hz, 1H), 3.75 (s, 3H), 3.13 (ddd, J = 15.4, 5.3, 1.2 Hz, 1H), 3.00 (ddd, J = 15.4, 7.4, 1.5 Hz, 1H), 1.96 (dddt, J = 15.0, 6.6, 4.6, 2.3 Hz, 2H), 1.88 (s, 2H), 1.73 (ddd, J = 13.7, 9.9, 4.8 Hz, 1H), 1.53 (ddd, J = 13.8, 9.4, 4.2 Hz, 1H), 1.04 (d, J = 6.5 Hz, 3H), 1.01 (d, J = 6.7 Hz, 3H). ^{13}C NMR (101 MHz, CDCl$_3$) δ 174.4, 136.0, 135.9, 127.2, 121.7, 119.5, 118.1, 110.8, 106.8, 52.5, 52.2, 48.2, 44.5, 25.1, 24.8, 23.8, 21.7. This compound has been previously reported and NMR data are consistent with literature.[64]

Methyl (1*R*,3*S*)-1-isobutyl-2,3,4,9-tetrahydro-1*H*-pyrido[3,4-*b*]indole-3-carboxylate (8ae): ^{1}H NMR (400 MHz, CDCl$_3$) δ 7.84 (s, 1H), 7.48 (ddt, J = 7.6, 1.5, 0.7 Hz, 1H), 7.33 – 7.30 (m, 1H), 7.19 – 7.14 (m, 1H), 7.11 (ddd, J = 7.1, 1.3 Hz, 1H), 4.23 (ddt, J = 9.0, 4.4, 2.2 Hz, 1H), 3.83 (s, 3H), 3.80 (dd, J = 11.2, 4.2 Hz, 1H), 3.14 (ddd, J = 15.0, 4.2, 1.9 Hz, 1H), 2.83 (ddd, J = 15.0, 11.2, 2.6 Hz, 1H), 2.10 – 1.97 (m, 2H), 1.75 – 1.60 (m, 2H), 1.04 (d, J = 6.6 Hz, 3H), 1.01 (d, J = 6.6 Hz, 3H). ^{13}C NMR (101 MHz, CDCl$_3$) δ 173.9, 136.2, 136.0, 127.4, 121.8, 119.7, 118.1, 110.9, 107.9, 56.6, 52.3, 50.7, 44.5, 26.1, 24.4, 24.0, 21.8. This compound has been previously reported and NMR data are consistent with literature.[64]

Supplementary Material

Refer to Web version on PubMed Central for supplementary material.

Acknowledgements

Notes and references

1. Laine AE, Lood C and Koskinen AMP, Molecules, 2014, 19, 1544–1567. [PubMed: 24473212]

2. Beghyn TB, Charton J, Leroux F, Laconde G, Bourin A, Cos P, Maes L and Deprez B, J. Med. Chem, 2011, 54, 3222–3240. [PubMed: 21504142]

3. Cox ED and Cook JM, Chem. Rev, 1995, 95, 1797–1842.

4. Rahman MT, Deschamps JR, Imler GH and Cook JM, Chem-Eur J, 2018, 24, 2354–2359. [PubMed: 29244896]

5. Daugan A, Grondin P, Ruault C, Le A-C de Gouville Monnier, Coste H, Linget JM, Kirilovsky J, Hyafil F and Labaudinière R, J. Med. Chem, 2003, 46, 4533–4542. [PubMed: 14521415]

6. De Savi C, Bradbury RH, Rabow AA, Norman RA, de Almeida C, Andrews DM, Ballard P, Buttar D, Callis RJ, Currie GS, Curwen JO, Davies CD, Donald CS, Feron LJL, Gingell H, Glossop SC, Hayter BR, Hussain S, Karoutchi G, Lamont SG, MacFaul P, Moss TA, Pearson SE, Tonge M, Walker GE, Weir HM and Wilson Z, J. Med. Chem, 2015, 58, 8128–8140. [PubMed: 26407012]

7. Bowman JD, Merino EF, Brooks CF, Striepen B, Carlier PR and Cassera MB, Antimicrob. Agents. Chemother, 2014, 58, 811–819. [PubMed: 24247137]

8. Spangenberg T, Burrows JN, Kowalczyk P, McDonald S, Wells TNC and Willis P, PLOS One, 2013, 8, e62906. [PubMed: 23798988]

9. Yao Z-K, Krai PM, Merino EF, Simpson ME, Slebodnick C, Cassera MB and Carlier PR, Bioorg. Med. Chem. Lett, 2015, 25, 1515–1519. [PubMed: 25754494]

10. Wu W, Herrera Z, Ebert D, Baska K, Cho SH, DeRisi JL and Yeh E, Antimicrob. Agents. Chemother, 2015, 59, 356–364. [PubMed: 25367906]

11. Imlay LS, Armstrong CM, Masters MC, Li T, Price KE, Edwards R, Mann KM, Li LX, Stallings CL, Berry NG, O'Neill PM and Odom AR, ACS Infect. Dis, 2015, 1, 157–167. [PubMed: 26783558]

12. Ungemach F, Soerens D, Weber R, DiPierro M, Campos O, Mokry P, Cook JM and Silverton JV, J. Am. Chem. Soc, 1980, 102, 6976–6984.

13. Bringmann G, Hille A, Stablein M, Peters K and Vonschnering HG, Liebigs Ann. Chem, 1991, 1189–1194.

14. Alberch L, Bailey PD, Clingan PD, Mills TJ, Price RA and Pritchard RG, Eur. J. Org. Chem, 2004, DOI: 10.1002/ejoc.200400017, 1887–1890.

15. Alam S, Hasan M, Saeed S, Fischer A and Khan N, Acta Cryst. Sect. E-Struc. Rep . Online, 2007, 63, O871–O872.

16. Pulka K, Kulis P, Tymecka D, Frankiewicz L, Wilczek M, Kominski W and Misicka A, Tetrahedron, 2008, 64, 1506–1514.

17. Xiao S, Lu X, Shi X-X, Sun Y, Liang L-L, Yu X-H and Dong J, Tetrahedron: Asymmetry, 2009, 20, 430–439.

18. Mohamed HA, Girgis NMR, Wilcken R, Bauer MR, Tinsley HN, Gary BD, Piazza GA, Boeckler FM and Abadi AH, J. Med. Chem, 2011, 54, 495–509. [PubMed: 21189023]

19. Duddeck H, in Topics in Stereochemistry, ed. Eliel EL, Wilen SH, Allinger NL, John Wiley & Sons, Inc., 1986, vol. 16, pp. 219–324.

20. For an excellent brief summary, seeReich Hans J., 2010, "Carbon-13 Nuclear Magnetic Resonance Spectroscopy", p. 6-CMR-4–3 to 6-CMR-4–5, https://www.chem.wisc.edu/areas/reich/nmr/notes-6-cmr.pdf last accessed 4/17/19.

21. Dalling DK, Grant DM and Paul EG, J. Am. Chem. Soc, 1973, 95, 3718–3724.

22. Clemans GB and Alemayehu M, Tetrahedron Lett, 1993, 34, 1563–1566.

23. Rychnovsky SD and Skalitzky DJ, Tetrahedron Lett, 1990, 31, 945–948.

24. Schneider HJ and Hoppen V, J. Org. Chem, 1978, 43, 3866–3873.

25. Manoharan M and Eliel EL, Magn. Res. Chem, 1985, 23, 225–231.

26. Buchanan GW, Can. J. Chem.-Rev. Can. Chim, 1982, 60, 2908–2913.

27. Buchanan GW, Preusser SH and Webb VL, Can. J. Chem.-Rev. Can. Chim, 1984, 62, 1308–1311.

28. Zhang H and Timmermann BN, J. Nat. Prod, 2016, 79, 732–742. [PubMed: 26894655]

29. Hoffmann RW and Froech S, Tetrahedron Lett, 1985, 26, 1643–1646.

30. Hoffmann RW and Weidmann U, Chem. Ber.-Recl, 1985, 118, 3980–3992.

31. Heathcock CH, Pirrung MC and Sohn JE, J. Org. Chem, 1979, 44, 4294–4299.

32. Peter A, Vaughan-Williams GF and Rosser RM, Tetrahedron, 1993, 49, 3007–3034.

33. Jung S and Podlech J, J. Phys. Chem. A, 2018, 122, 5764–5772. [PubMed: 29894191]

34. Ungemach F, DiPierro M, Weber R and Cook JM, J. Org. Chem, 1981, 46, 164–168.

35. Bailey PD, Hollinshead SP, McLay NR, Morgan K, Palmer SJ, Prince SN, Reynolds CD and Wood SD, Journal of the Chemical Society, Perkin Transactions 1, 1993, DOI: 10.1039/p19930000431, 431–439.

36. Rahman MT and Cook JM, Eur. J. Org. Chem, 2018, DOI: 10.1002/ejoc.201800600, 3224–3229.

37. Ghavami M, Merino EF, Yao Z-K, Elahi R, Simpson ME, Fernández-Murga ML, Butler JH, Casasanta MA, Krai PM, Totrov MM, Slade DJ, Carlier PR and Cassera MB, ACS Infect. Dis, 2018, 4, 549–559. [PubMed: 29072835]

38. Note that Ungemach et al. (ref. 12) did not draw this conclusion; instead they proposed the trans-configured compounds would exclusively adopt an ψeq-CO2Me conformation (conformer B, Figure 3) to relieve allylic strain between the 1-aryl group and the indole NH. Bringmann (ref 13) and Pulka (ref 16) reached the same conclusions we proposed.

39. We note that Nakamura et al. made a similar analysis to assign relative stereochemistry in the reduction of dihydro-β-carbolines:Nakamura T, Ishida A,. Irie K, and Oh-ishi T Chem. Pharm. Bull 1984, 32, 2859–2862.

40. Günther H and Jikeli G, Chem. Rev, 1977, 77, 599–637.

41. Barfield M and Sternhell S, J. Am. Chem. Soc, 1972, 94, 1905–1913.

42. Becke A, J. Chem. Phys, 1993, 98, 5648–5652.

43. Lee CT, Yang WT and Parr RG, Phys. Rev. B, 1988, 37, 785–789.

44. The decidedly non-linear intramolecular hydrogen bonds seen in these structures (e.g. I, II in Figure 6) reflect electrostatic interaction between N-H and the ester oxygens, without the $n \rightarrow \sigma^*$ orbital overlap that can be realized in linear hydrogen bonds. See "3.2.3 Hydrogen Bonding" in "Modern Physical Organic Chemistry,"Anslyn EV, Dougherty DA, University Science Books, Sausalito CA, USA, 2006, p. 168–180.

45. See depictions of conformers 8a-4, 8a-8, 8a-9, 8a-12 to 8a-14 in the ESI.

46. Pettersen EF, Goddard TD, Huang CC, Couch GS, Greenblatt DM, Meng EC and Ferrin TE, J. Comput. Chem, 2004, 25, 1605–1612. [PubMed: 15264254]

47. Adamo C and Barone V, J. Chem. Phys, 1998, 108, 664–675.

48. Miertus S, Scrocco E and Tomasi J, Chem. Phys, 1981, 55, 117–129.

49. Pierens GK, Venkatachalam TK and Reutens DC, Sci. Rep, 2017, 7, 5605. [PubMed: 28717218]

50. Zhao Y and Truhlar D, Theor Chem Acc, 2008, 120, 215–241.

51. Zhao Y and Truhlar DG, Chem. Phys. Lett, 2011, 502, 1–13.

52. Weigend F and Ahlrichs R, Physical Chemistry Chemical Physics, 2005, 7, 3297–3305. [PubMed: 16240044]

53. Aliev AE, Karu K, Mitchell RE and Porter MJ, Org. Biomol. Chem, 2016, 14, 238–245. [PubMed: 26517805]

54. As noted above, at M06–2X/def2-TZVP (PCM,CHCl$_3$)//B3LYP/6–31G(d), 8a and 8b show less energetic differentiation of the ψ_{eq}- and ψ_{ax}-CO2Me conformations, populating only 80 and 94% of the ψ_{eq}-CO$_2$Me conformation A (Figure 3) respectively.

55. Friebolin H, in Basic One- and Two-Dimensional NMR Spectroscopy, Wiley-VCH, 1998, ch. 3, pp. 85–88.

56. Bally T and Rablen PR, J. Org. Chem, 2011, 76, 4818–4830. [PubMed: 21574622]

57. Except for molecular mechanics and semi-empirical models, the calculation methods used in Spartan have been documented in:Shao Y, Molnar LF, Jung Y, Kussmann J, Ochsenfeld C, Brown ST, Gilbert ATB, Slipchenko LV, Levchenko SV, O'Neill DP, DiStasio RA Jr., Lochan RC, Wang T, Beran GJO, Besley NA, Herbert JM, Lin CY, Van Voorhis T, Chien SH, Sodt A, Steele RP, Rassolov VA, Maslen PE, Korambath PP, Adamson RD, Austin B, Baker J, Byrd EFC, Dachsel H,

Doerksen RJ, Dreuw A, Dunietz BD, Dutoi AD, Furlani TR, Gwaltney SR, Heyden A, Hirata S, Hsu C-P, Kedziora G, Khalliulin RZ, Klunzinger P, Lee AM, Lee MS, Liang WZ, Lotan I, Nair N, Peters B, Proynov EI, Pieniazek PA, Rhee YM, Ritchie J, Rosta E, Sherrill CD, Simmonett AC, Subotnik JE, Woodcock III HL, Zhang W, Bell AT, Chakraborty AK, Chipman DM, Keil FJ, Warshel A, Hehre WJ, Schaefer HF, Kong J, Krylov AI, Gill PMW and Head-Gordon M, Phys. Chem. Chem. Phys, 2006, 8, 3172. [PubMed: 16902710]

58. Gaussian 09, Revision E.01,Frisch MJ, Trucks GW, Schlegel HB, Scuseria GE, Robb MA, Cheeseman JR, Scalmani G, Barone V, Mennucci B, Petersson GA, Nakatsuji H, Caricato M, Li X, Hratchian HP, Izmaylov AF, Bloino J, Zheng G, Sonnenberg JL, Hada M, Ehara M, Toyota K, Fukuda R, Hasegawa J, Ishida M, Nakajima T, Honda Y, Kitao O, Nakai H, Vreven T, Montgomery JA Jr, Peralta JE, Ogliaro F, Bearpark M, Heyd JJ, Brothers E, Kudin KN, Staroverov VN, Keith T, Kobayashi R, Normand J, Raghavachari K, Rendell A, Burant JC, Iyengar SS, Tomasi J, Cossi M, Rega N, Millam JM, Klene M, Knox JE, Cross JB, Bakken V, Adamo C, Jaramillo J, Gomperts R, Stratmann RE, Yazyev O, Austin AJ, Cammi R, Pomelli C, Ochterski JW, Martin RL, Morokuma K, Zakrzewski VG, Voth GA, Salvador P, Dannenberg JJ, Dapprich S, Daniels AD, Farkas O, Foresman JB, Ortiz JV, Cioslowski J, and Fox DJ, Gaussian, Inc., Wallingford CT, 2013.

59. Lodewyk MW, Siebert MR and Tantillo DJ, Chem. Rev, 2012, 112, 1839–1862. [PubMed: 22091891]

60. Saiga Y, Iijima I, Ishida A, Miyagishima T, Takamura N, Ohishi T, Matsumoto M and Matsuoka Y, Chem. Pharm. Bull, 1987, 35, 3705–3712. [PubMed: 3435969]

61. Soerens D, Sandrin J, Ungemach F, Mokry P, Wu GS, Yamanaka E, Hutchins L, DiPierro M and Cook JM, J. Org. Chem, 1979, 44, 535–545.

62. Bondzic BP and Eilbracht P, Org. Biomol. Chem, 2008, 6, 4059–4063. [PubMed: 18931815]

63. Ishida A, Nakamura T, Irie K and Ohishi T, Chem. Pharm. Bull, 1985, 33, 3237–3249.

64. Nakagawa M, Fukushima H, Kawate T, Hongu M, Une T, Kodato S, Taniguchi M and Hino T, Chem. Pharm. Bull, 1989, 37, 23–32.
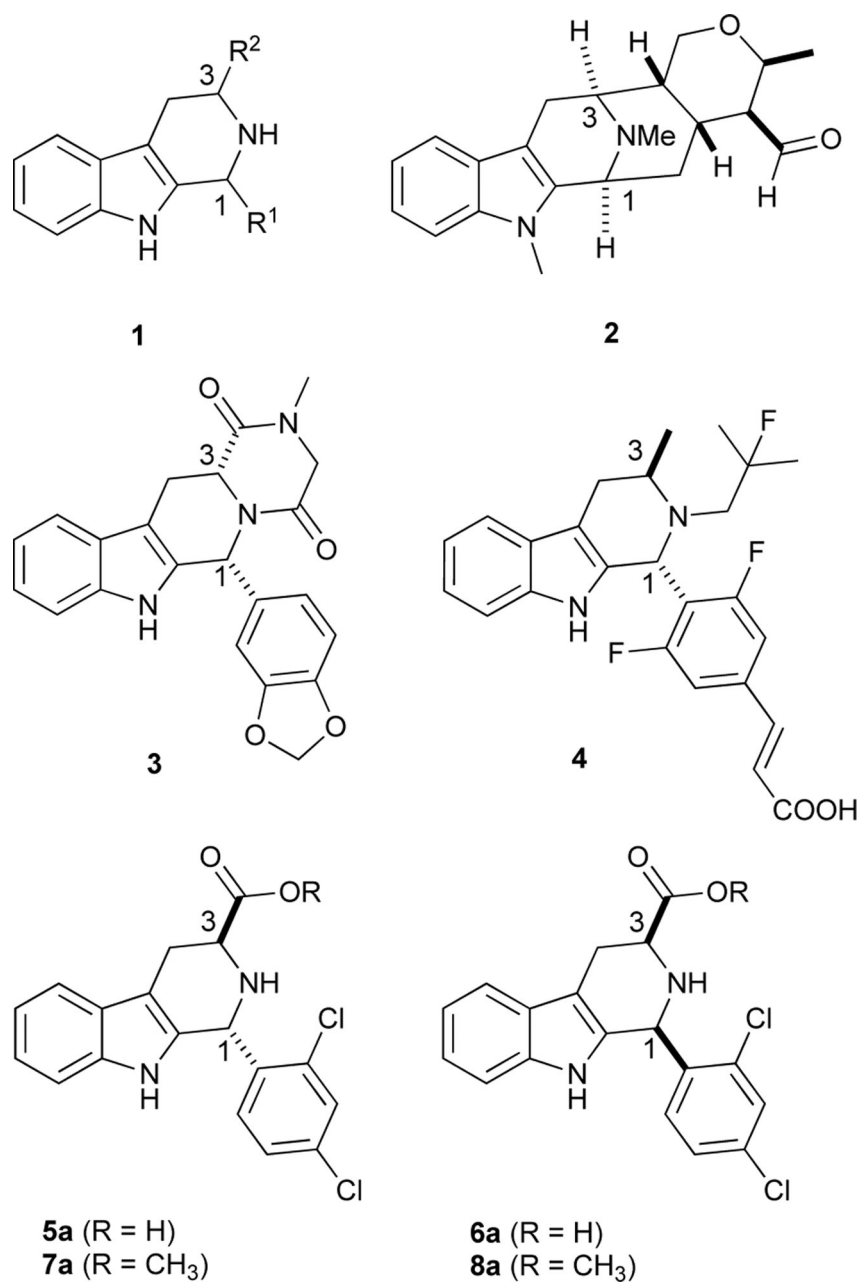
Figure 1.
1,3-disubsubstituted THβC **1** and related medicinally important compounds. Talcarpine's (**2**) atom numbering modified to highlight similarity to other THβCs in the Figure.
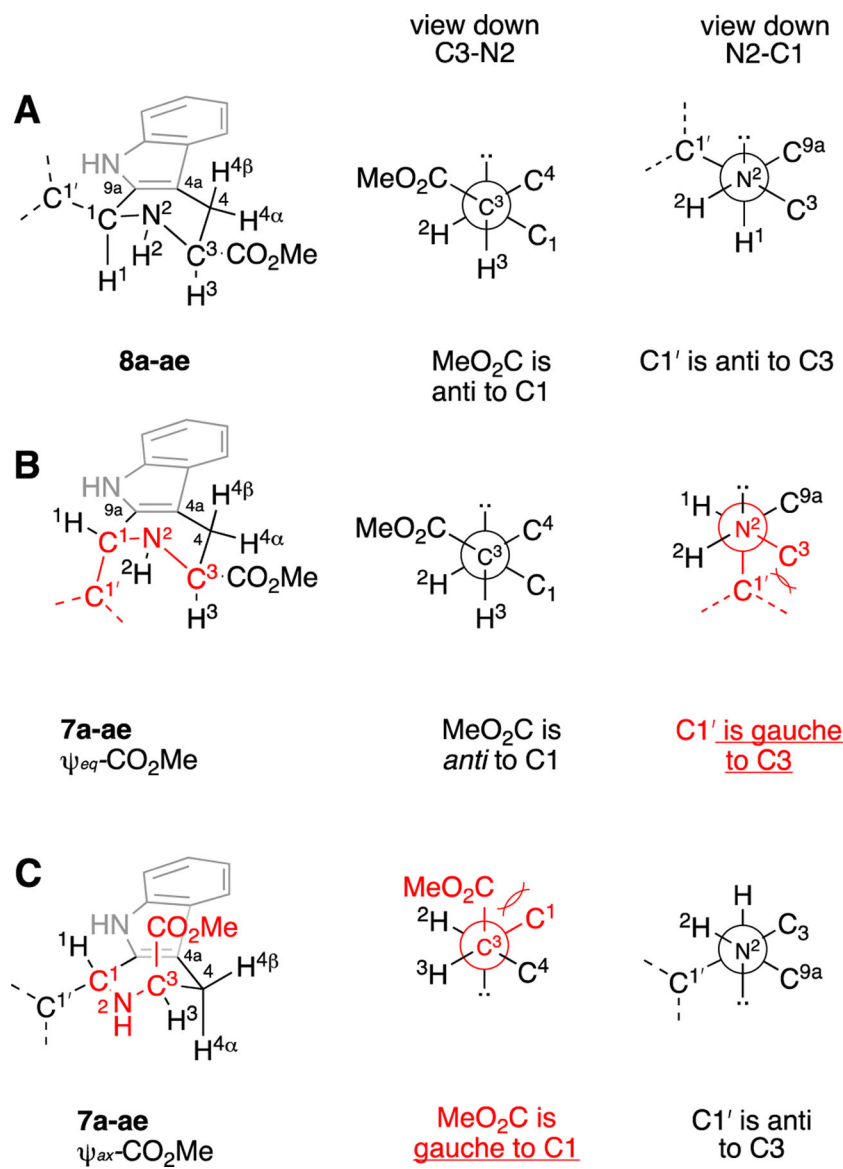
Figure 2.
Pictet-Spengler adduct methyl esters studied in this work.[9, 37]
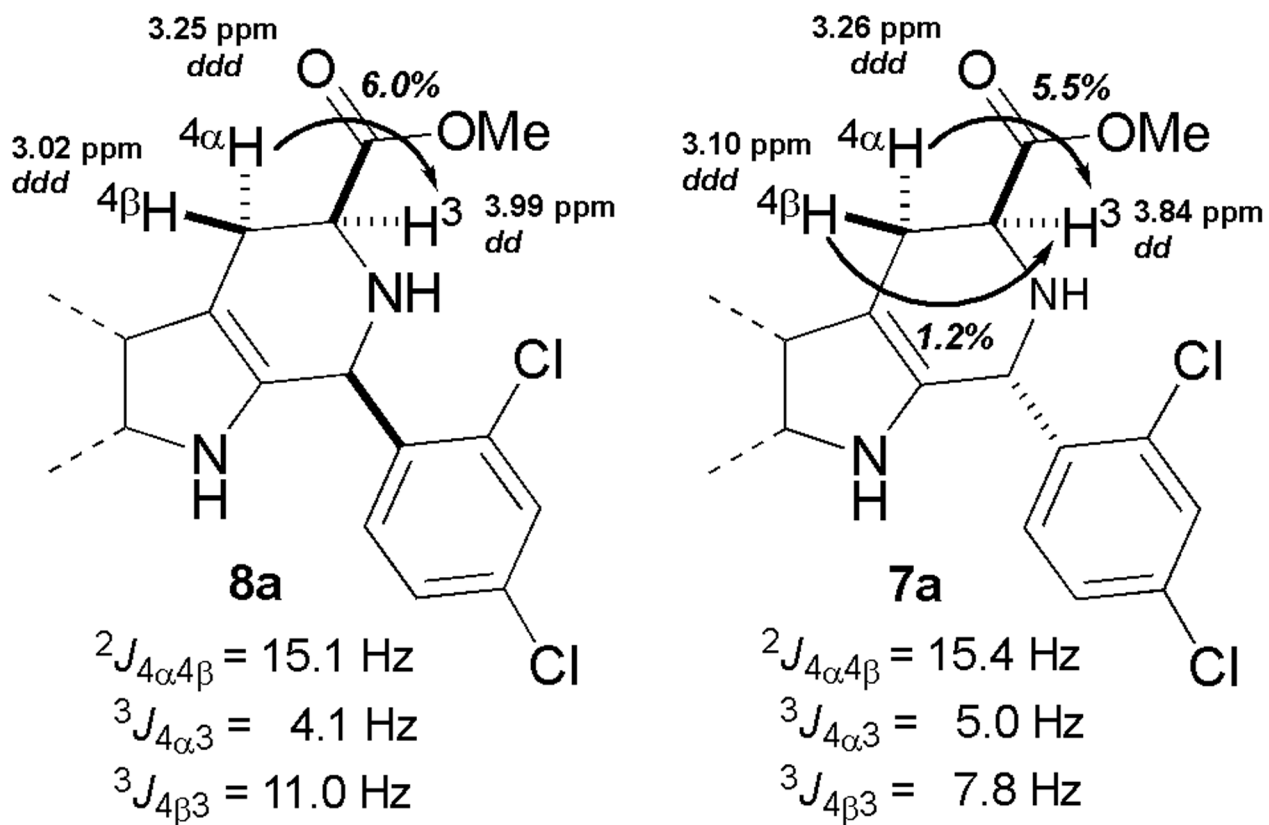
Figure 3.
Proposed half-chair conformations of the tetrahydropyridine rings in **8a-ae** (**A**) and **7a-ae** (**B**, **C**), and Newman projections down the C3-N2 and N2-C1 axes. Gauche interactions of ring substituents are highlighted in red.

Figure 4.
Assignment of diastereotopic protons H4α and H4β in **8a** and **7a**. Abbreviations used: dd = doublet of doublet, ddd = doublet of doublet of doublet. Note that H4α and H4β are coupled through 5 bonds to H1 (not shown), see Figure 5.
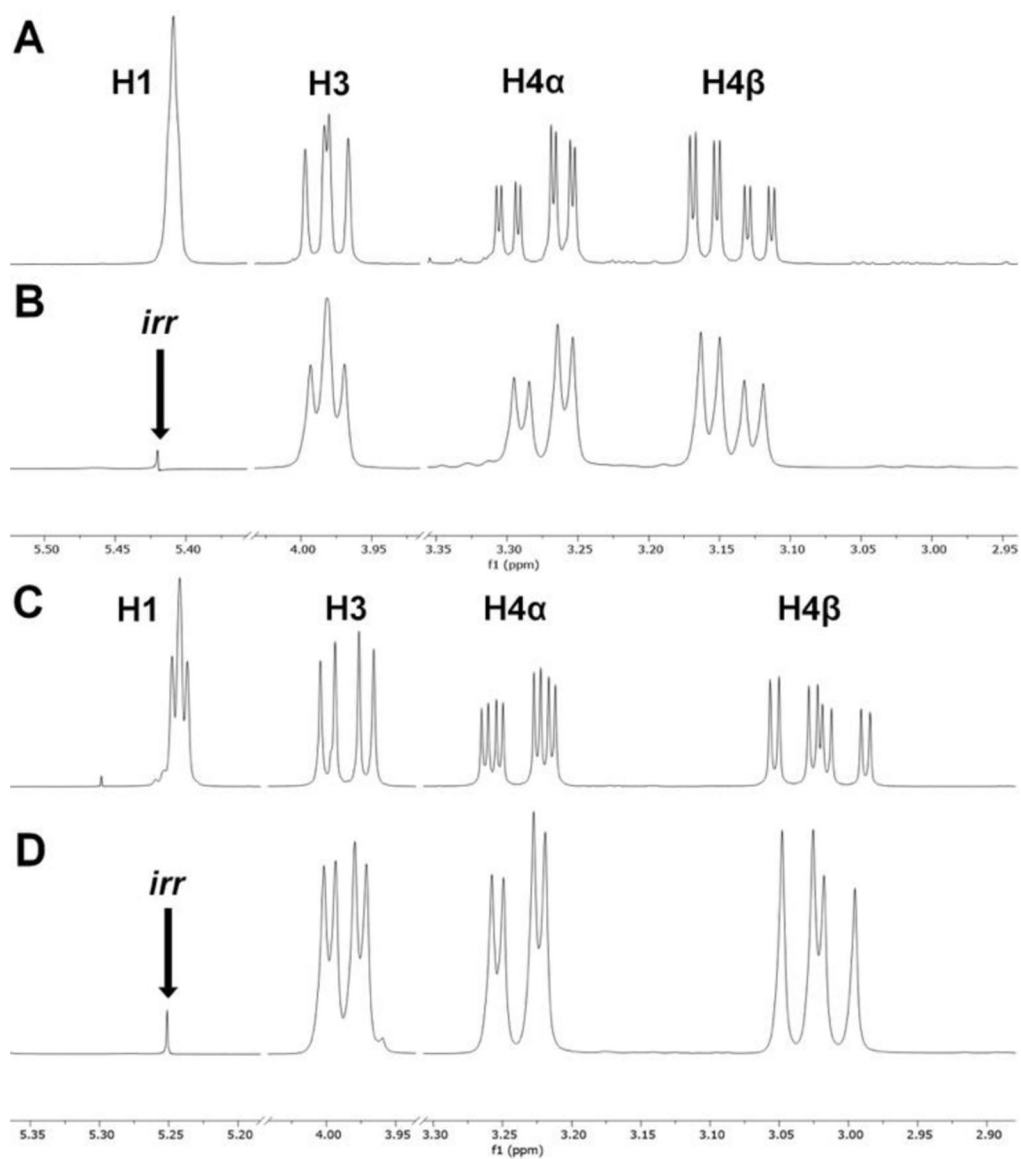
Figure 5.
Five-bond coupling of H1 to H4α and H4β in **7b** and **8b** A) H1, H3, H4α, and H4β resonances in the ^{1}H NMR spectrum of **7b**; B) Single frequency decoupling of H1 in **7b**; C) H1, H3, H4α, and H4β resonances in the ^{1}H NMR spectrum of **8b**; D) Single frequency decoupling of H1 in **8b**.
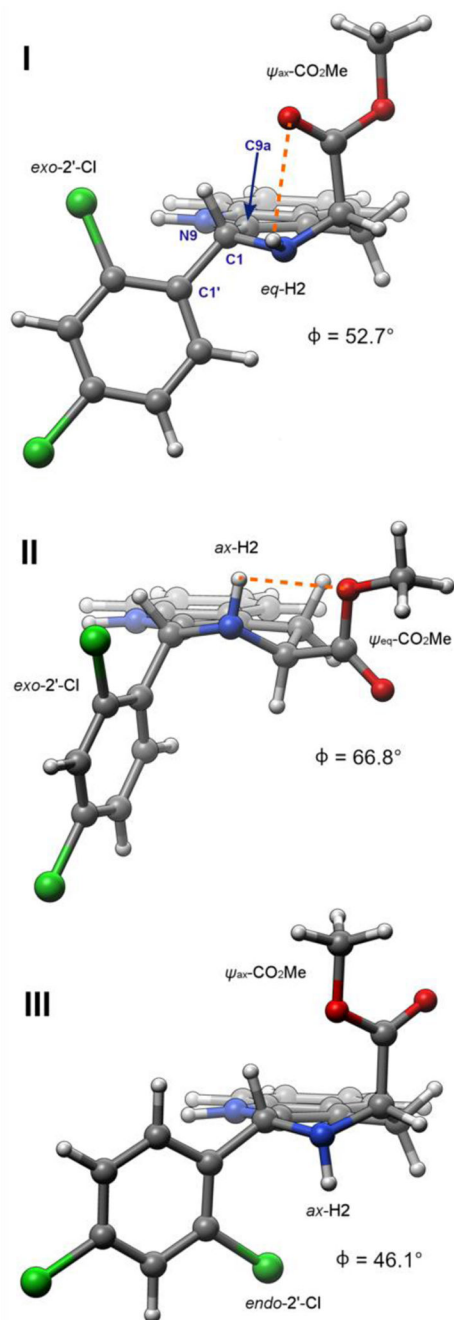
Figure 6.
Representative calculated (B3LYP/6–31G(d)) structures of **7a** illustrating the orientation of the CO_2Me, NH, and 2'-Cl groups. The C1-C1-C9a-N9 dihedral angle is represented by φ. In conformers **I** and **II**, internal hydrogen bonding between H2 and the carbonyl or methoxy O atoms is depicted with orange dashed line. Note that intramolecular hydrogen bonding is geometrically impossible in conformer **III**. Conformers **I**, **II**, and **III** are described as **7a**-01, **7a**-09, and **7a**-10 respectively in the Supporting Information. Graphics rendered using Chimera.[46]

Figure 7.
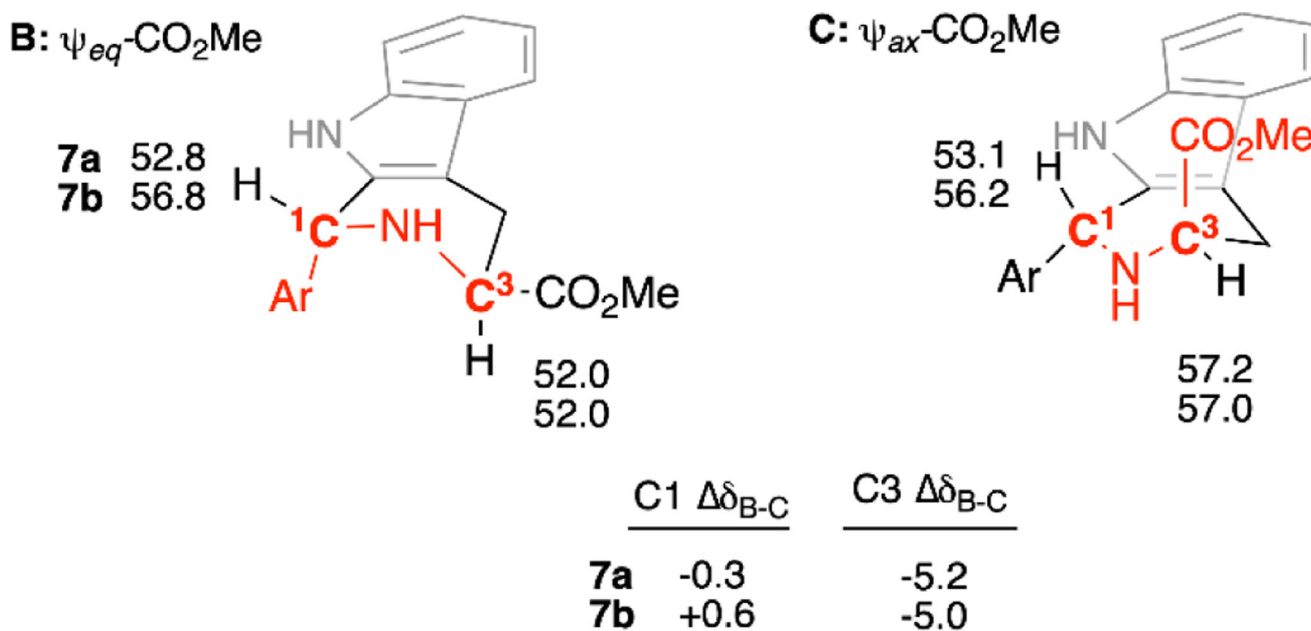Weighted (mPW1PW91/6–311+G(2d,p) (PCM,CHCl$_3$)//B3LYP/6–31G(d)) ^{13}C NMR chemical shifts for C1 & C3 of **7a** and **7b** in the ψ_{eq}- and ψ_{ax}-CO$_2$Me tetrahydropyridine conformational ensembles **B** and **C**. Gauche interactions of ring substituents with C1 and C3 are highlighted in red.

Table 1

Average ^{13}C NMR chemical shifts (δ, ppm) of C3, C1, C=O, and C1' (CDCl$_3$) in the *trans*- and *cis*-Pictet-Spengler adducts (**7a-7ae** and **8a-8ae**, respectively), and average relative shifts of the *trans*-adducts (δ_{7-8}, ppm).

	δ(7a-ae)	δ(8a-ae)	$\delta_{7-8}{}^{a}$
C3	52.5 ± 0.6	56.8 ± 0.2	-4.1 ± 0.6
C1	51.7 ± 3.2	54.6 ± 3.4	-2.9 ± 0.5
C=O	174.0 ± 0.4	173.3 ± 0.2	$+0.8 \pm 0.2$
Aryl C1'^{b}	134.2 ± 7.8	133.4 ± 8.2	$+0.9 \pm 0.5$
Alkyl C1'^{c}	41.4 ± 4.7	40.7 ± 5.2	$+0.7 \pm 0.4$

^{a}Defined at each of the carbons as δ for **7** – δ for **8**.

^{b}Data from 16 1-aryl Pictet-Spengler analogs for which C1' was unambiguously assigned.

^{c}Data from **7aa-ae** and **8aa-ae**.

Table 2

Selected average ^{1}H chemical shifts and coupling constants in **7a**-**ae** and **8a**-**ae** (CDCl$_3$).

Entry	Avg	7a-ae	8a-ae
1	δ H3 (ppm)	3.91 ± 0.09	3.94 ± 0.09
2	δ H4α (ppm)	3.23 ± 0.06	3.22 ± 0.04
3	δ H4β (ppm)	3.10 ± 0.05	2.98 ± 0.08
4	$^3J_{4\beta-3}$ (Hz)	7.3 ± 0.9	11.1 ± 0.1
5	$^3J_{4\alpha-3}$ (Hz)	5.2 ± 0.2	4.1 ± 0.1
6	$^2J_{4\alpha-4\beta}$ (Hz)	15.3 ± 0.1	15.1 ± 0.1
7	$^5J_{4\beta-1}$ (Hz)	1.5 ± 0.1	2.5 ± 0.1
8	$^5J_{4\alpha-1}$ (Hz)	1.3 ± 0.2	1.8 ± 0.1

Table 3

The number of B3LYP/6–31G(d) potential energy minima found for **7a**/**8a**, **7b**/**8b** within each conformational ensemble.

Conformer	7a	8a	7b	8b
Total	16	14	8	8
ψ_{ax}-CO$_2$Me	8	6	4	4
ψ_{eq}-CO$_2$Me	8	8	4	4
exo-2'-Cl	8	8	-	-
endo-2'-Cl	8	6[a]	-	-
ax-H2	8	6	4	4
eq-H2	8	8	4	4
H-bond[b]	12	12	6	6
No H-bond[c]	4	4	2	2

[a] Two conformers, namely ψ_{ax}-CO$_2$Me, *endo*-2'-Cl, *ax*-H2, were not found in the initial conformational search, likely due to their expected high energy.

[b] Intramolecular H-bonding of H2 to C=O or OMe deduced from H2⋯O distances ranging from 2.3 – 2.7 Å.

[c] Lack of H-bond deduced from H2⋯O > 3.7 Å.

Table 4

Boltzmann distribution of conformational ensembles, based on mPW1PW91/6–311+G(2d,p) (PCM, CHCl$_3$)// B3LYP/6–31G(d) free energies at 298 K.

| | 7a | 8a | 7b | 8b |
	[%]	[%]	[%]	[%]
ψ_{ax}-CO$_2$Me	26.9	2.6	39.8	0.8
ψ_{eq}-CO$_2$Me	73.1	97.4	60.2	99.2
exo-2'-Cl	93.0	81.7	–	–
endo-2'-Cl	7.0	18.3	–	–
ax-H2	38.6	47.8	35.9	42.5
eq-H2	61.4	52.2	64.1	57.5
H-bond	95.0	99.5	94.2	99.9
No H-bond	5.0	0.5	5.8	0.1

Table 5

Calculated (B3LYP/6–31(d,p)u+1s//B3LYP/6–31G(d))[a] vs observed (italics) ^{1}H-^{1}H coupling constants for **7a/8a** and **7b/8b**.

	7a	8a	7b	8b
	(Hz)	(Hz)	(Hz)	(Hz)
$^3J_{4\beta-3}$	8.3/*7.8*	10.5/*11.0*	6.2/*6.8*	10.7/*11.2*
$^3J_{4\alpha-3}$	4.5/*5.0*	3.9/*4.1*	5.1/*5.4*	3.9/*4.3*
$^2J_{4\alpha-4\beta}$ [b]	15.3/*15.4*	15.1/*15.1*	15.3/*15.4*	15.0/*15.2*
$^5J_{4\beta-1}$	1.9/*1.5*	3.0/*2.5*	1.9/*1.6*	3.0/*2.6*
$^5J_{4\alpha-1}$	1.2/*1.2*	2.0/*1.9*	1.8/*1.4*	2.1/*1.9*

[a] Weighted average over all conformations, based on mPW1PW91/6–311+G(2d,p)//B3LYP/6–31G(d) Boltzmann distribution (298 K).

[b] $^2J_{HH}$ values for sp^3 C-H are calculated to be negative, as expected;[55] the absolute values are shown here.

Table 6

All-carbon mean absolute deviation (MAD) in calculated ^{13}C NMR chemical shifts for **7a**, **7b**, **8a**, and **8b** at the indicated levels of theory.

Compound	B3LYP/6–311+G(2d,p) (PCM, CHCl₃)// B3LYP/6–31G(d) (ppm)[a]	mPW1PW91/6–311+G(2d,p) (PCM, CHCl₃)// B3LYP/6–31G(d) (ppm)[a]
7a	2.1	1.7
7b	1.5	1.1
8a	2.0	1.6
8b	1.4	1.0
Average[b]	1.8	1.4

[a]Mean absolute deviation in ^{13}C NMR chemical shift for all 19 carbons in each compound.

[b]Average of MAD for compounds **7a**, **7b**, **8a**, and **8b**.

Table 7

Calculated[a] *vs* observed (italics) ^{13}C NMR chemical shifts (δ) for select carbons in **7a**, **7b**, **8a**, **8b**, and corresponding differences in δ between diastereomers (δ$_{7-8}$).

Carbon	Compounds	δ(7)	δ(8)	δ$_{7-8}$[b]
C3	**7a**, **8a**	53.4 / *52.3*	57.5 / *56.7*	−4.1 / *−4.4*
	7b, **8b**	54.0 / *52.7*	57.8 / *57.0*	−3.8 / *−4.3*
C1	**7a**, **8a**	52.9 / *51.3*	55.8 / *53.9*	−2.9 / *−2.6*
	7b, **8b**	56.6 / *55.1*	59.8 / *58.8*	−3.2 / *−3.7*
C=O	**7a**, **8a**	175.3 / *173.8*	174.9 / *173.1*	+0.4 / *+0.7*
	7b, **8b**	175.8 / *174.3*	175.1 / *173.3*	+0.7 / *+1.0*
C1'	**7a**, **8a**	139.2 / *137.9*	138.6 / *137.4*	+0.6 / *+0.5*
	7b, **8b**	143.8 / *142.1*	142.2 / *140.8*	+1.6 / *+1.3*

[a]Boltzmann Weighted mPW1PW91/6–311+G(2d,p) (PCM, CHCl3)//B3LYP/6–31G(d) ^{13}C NMR chemical shifts.

[b] δ$_{7-8}$ = δ(**7**) − δ(**8**); values in normal font are derived from calculated chemical shifts, values in italics are from observed chemical shifts.